# The baYes* software package for Bayesian analysis of superdense nuclear matter models

Alexander Ayriyan[1], Hovik Grigorian[1,2], Gevorg Poghosyan[3]

[1] Laboratory of Information Technologies, JINR, [2] Department of Theoretical Physics, YSU, Armenia, [3] Karlsruhe Institute of Technology, Germany

The software package "**B**ayesian **A**nalysis of **E**quation of **S**tate" (**ba**Y**es**) is devoted to the problem of defining and classification of the best models of equation of state (EoS) of superdense nuclear matter, which describe compact star characteristics from observations. The package uses the Bayesian method to calculate *a posteriori* probabilities of a set of hypotheses based on occasional data.

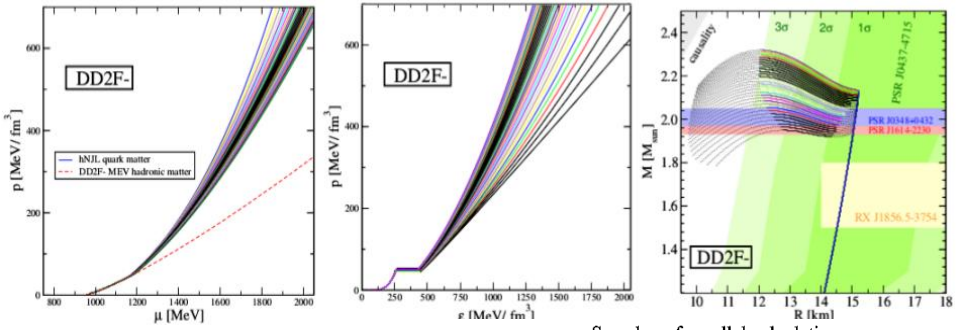


**Fig. 1. Variations of the hybrid EoS for the DD2F-NJL models for different model parameters (p - excluded volume, η4 - eight quark coupling) (left and central); the corresponding sequences of star configurations with observational constraints (right picture).**

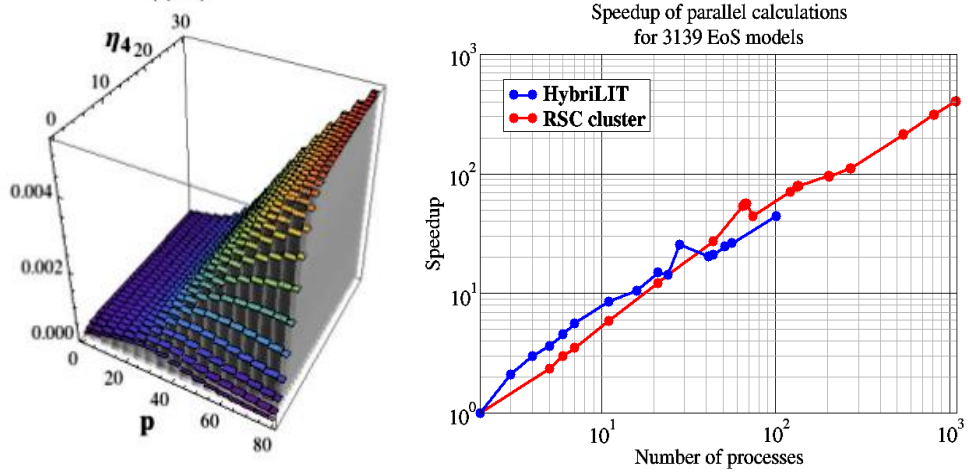


**Fig. 2. The distribution of the *a posteriori* probabilities of the EoS models with the given observational constraints (left). The the speedup of the parallel calculations for simulation of neutron star configurations (solving TOV equations) (right). Red line represents the result for new 4xIntel Xeon Phi 7250 using AVX512 (RSC cluster). Blue line is the result for 4xIntel Xeon E5-2695v3 using AVX2 (HybriLIT cluster)**

**D. Alvarez-Castillo, A. Ayriyan, S. Benic, D. Blaschke, H. Grigorian and S. Typel. *New class of hybrid EoS and Bayesian M-R data analysis* // Eur. Phys. J. A, 52:3 (2016) 69, doi: 10.1140/epja/i2016-16069-2**

# Smart Scheduler for the JINR Cloud

N. Balashov, A. Baranov, I. Kadochnikov, N. Kutovskiy, A. Nechaevskiy, I. Pelevanyuk

- The intention is to optimize cloud resources utilization efficiency
- A basic framework is designed
- Modular design
- Open-source
-

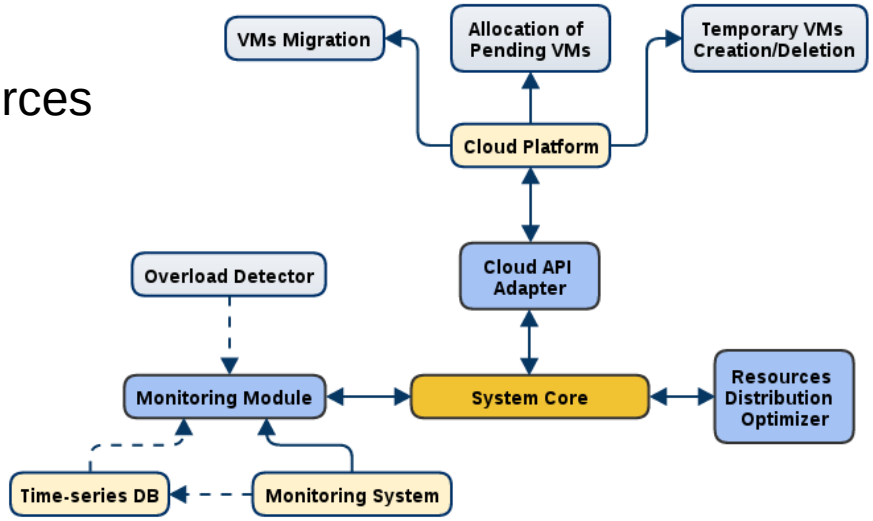


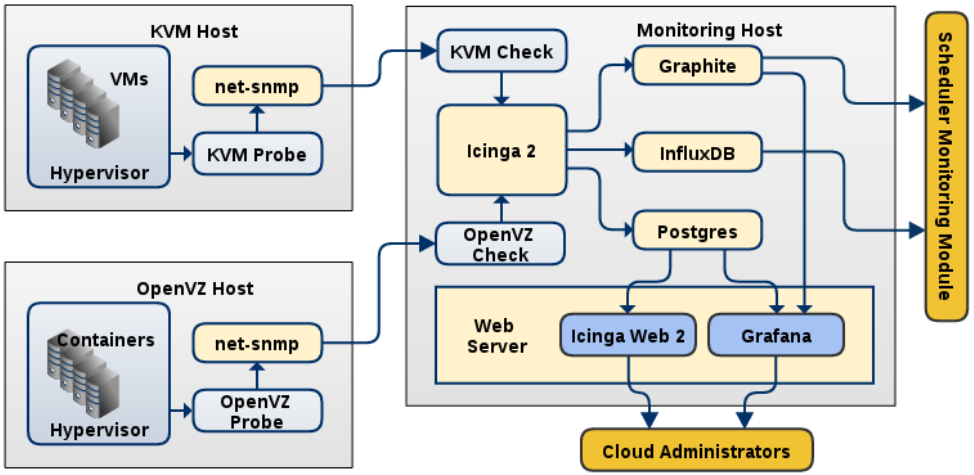


- Monitoring is a crucial part
- Development finished - commissioning
- Gives current system state
- Stores historical metrics
- Supports KVM and OpenVZ

# Simulation of radiation damage to different neuronal structures with Geant4-DNA toolkit

L. Bayarchimeg[1] , O.V. Belov[1], M. Batmunkh[1,2], O. Lkhagva[2]

*[1]Laboratory of Radiation Biology, JINR , [2] National University of Mongolia*

Cosmic rays

**Aim:**

- Development of computational methods for assessing the molecular mechanisms of synaptic receptors in CNS structural and functional disorders induced by ionizing radiations.

**Results:**

- This poster introduces newly developed simulation approach for neuronal microdosimetry. The geometries of neuronal receptors and neuronal network were constructed using experimental data on their molecule and cell morphologies, respectively.
- In the present works [1–3], investigated direct and indirect effects of radiation damage to a network of individual neurons and to glutamate receptors located in neuron synaptic zones.

A network of pyramidal neurons with 1 GeV/u $^{56}$Fe ions

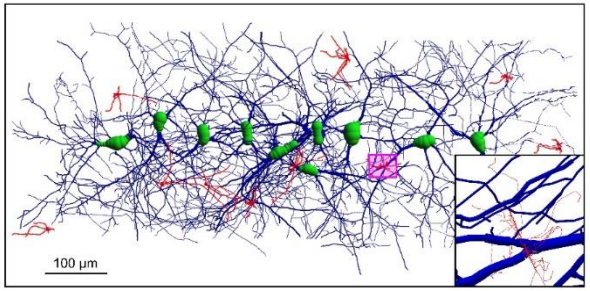


Track structure of a synapse with receptors induced by 0.1 GeV/u $^{56}$Fe ions

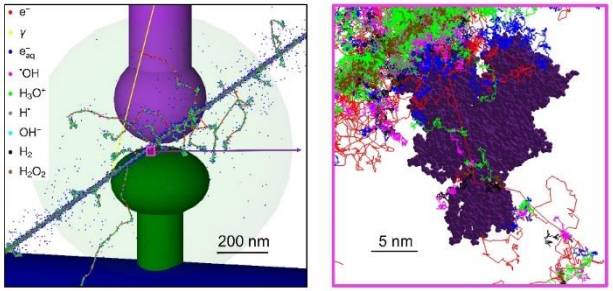


Scheme of simulation approach

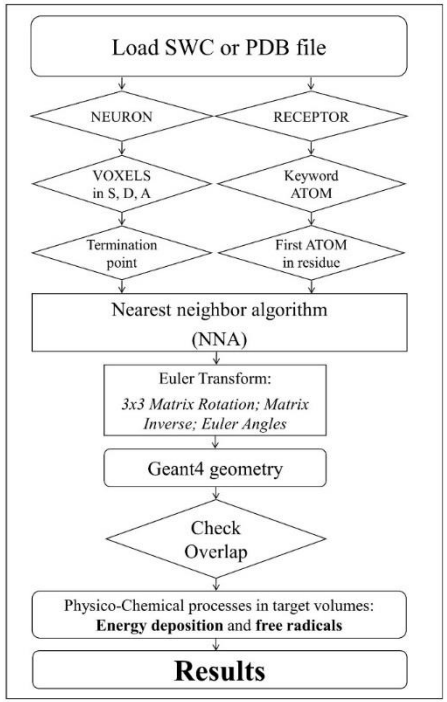


[1] M. Batmunkh, O.V. Belov, L. Bayarchimeg, et al., Estimation of the spatial energy deposition in CA1 pyramidal neurons under exposure to $^{12}$C and $^{56}$Fe ion beams, // Rad.Res.App.Sci, 2015. 8: 498-507.
[2] O. V. Belov, M. Batmunkh, S. Incerti, et al., Radiation damage to neuronal cells: Simulating the energy deposition and water radiolysis in a small neural network // Physica Medica, 2016. 32: 1510-1520.
[3] L. Bayarchimeg, O.V. Belov, M. Batmunkh, O. Lkhagva, Modeling of synaptic receptors under irradiation with charged particles // Mongolian Journal of Physics, 2016. (in press)

Тема 1103

# EFFECTS OF HYPOFRACTIONATED AND STANDARD FRACTIONATED IRRADIATION OF MICE HEADS WITH GAMMA - RAYS AND PROTONS ON THEIR PHERIPHERAL BLOOD PARAMETERS AND BEHAVIOR

K.Sh. Voskanyan[1], A.V. Rzyanina[1], D.M. Borowicz[1],[2], G.V.Mitsyn[1], V.N. Gaevsky[1], A.G. Molokanov[1]

1 Joint Institute for Nuvlear Research, Laboratory of Nuclear Problems, Dubna, Russia
2 Greater Poland Cancer Centre, Department of Medical Physics, Poznan, Poland

Rapporteur: Dorota Borowicz

**Abstract**: Experiments were performed to study the action of fractionated irradiation of mice heads with γ-rays and protons on their peripheral blood parameters and behavior by the "Open Field" test. Mice were irradiated in two variants of fractionated irradiation:
(1) traditional fractionation (in radiation therapy): 2 Gy once a day, 5 times a week, the total radiation dose 20 Gy;
(2) extreme hypofractionation: 10 Gy once a week, on Mondays, the total radiation dose 20 Gy.

The results of the study showed that irradiation of mice heads has no effect on their peripheral blood parameters in both variants of the applied fractionated irradiation and the behavior of mice does not depend on the type of ionizing radiation and the variant of fractionated exposure that we used. On the basis of these results it can be concluded that the option of extreme hypofractionation we have chosen can successfully replace traditional fractionation, which in some cases is applied when carrying out radiotherapy for treating brain tumors. The application of this type of fractionation can lead to shorter terms of radiotherapy and bigger patient capacity of medical centers that conduct radiotherapy.

# MICROSTRUCTURE AND RADIATION HARDENING STUDIES OF ODS STEELS FOR GENERATION IV NUCLEAR REACTORS

**K. Kornieieva[1], V. A. Skuratov[1], A. S. Sohatsky[1], J. O'Connell[2], Yu. I. Golovin[3], V.V. Korenkov[3], J. Neethling[2]**

[1]FLNR, JINR, Dubna, Russia, [2] CHRTEM NMMU, Port Elizabeth, South Africa, [3] TSU, Tambov, Russia

***Oxide dispersion strengthened (ODS)*** *steels are the most perspective structural materials for fuel cladding of Generation IV nuclear reactors.*

*The most interesting and less studied questions by now concern stability of the oxide structure during fission fragment impact and associated evolution of mechanical properties.*

## Structural examinations

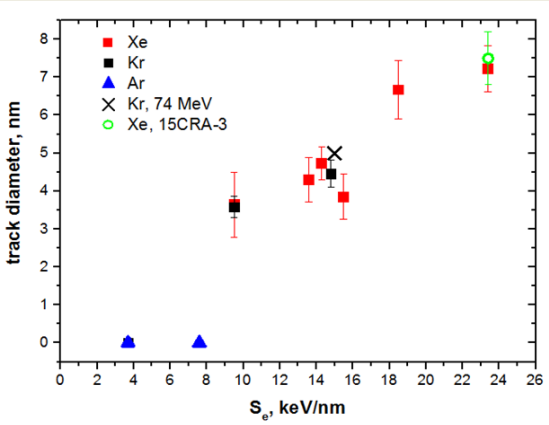


Latent track diameter as a function of $S_e$ for various ions in $Y_2Ti_2O_7$.

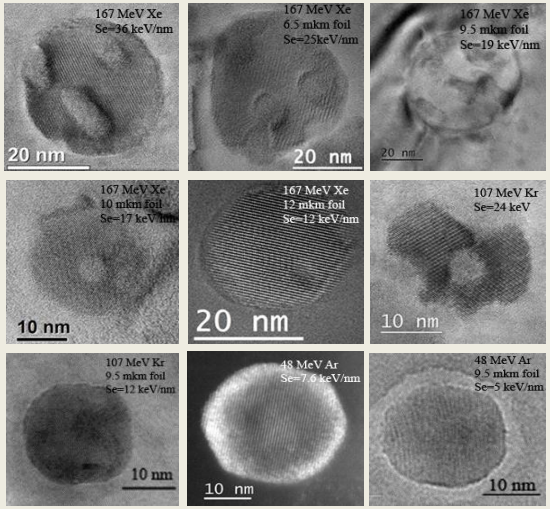


Latent tracks in $Y_2Ti_2O_7$.

## Mechanical properties

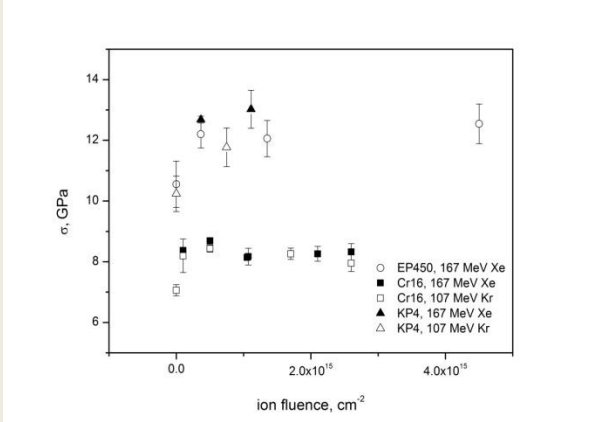


Yield stress vs. ion fluence for EP450, KP4 and Cr16 ODS steels.

*Dispersed barrier model:*

$$\Delta\sigma_{y,i} = \alpha_i M \mu b \sqrt{N_i d_i}$$

# Main directions of the JINR cloud evolution

**Integration of partner organizations' clouds**

· Nazarbaev University (Astana, Kazakhstan), work is in progress

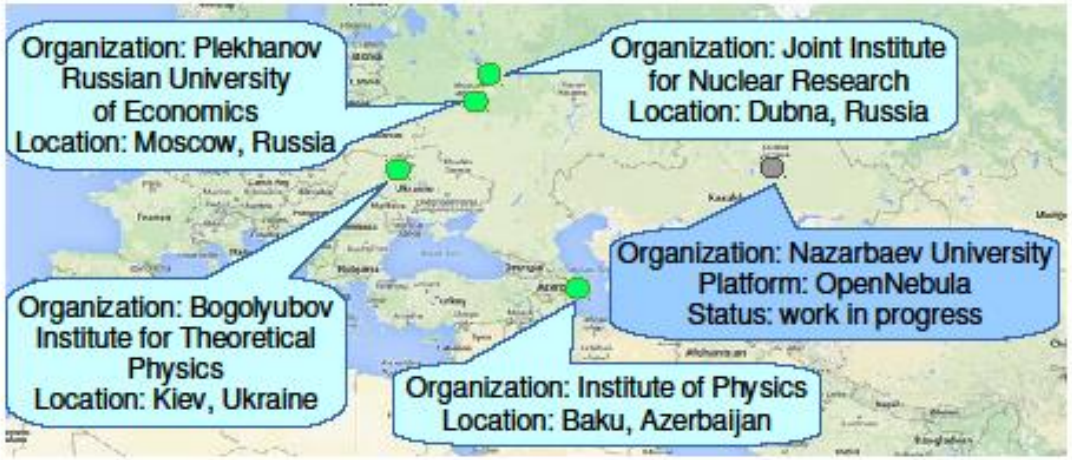


**Increasing resources**

- Total CPU cores: 400 (+200 during 2016)
- Total RAM: 980 GB (+580)
- Distributed network storage: 16 TB
- Total local HDDs capacity: 42 TB (+25 TB)
- Users: 115 (+35)
- Runnings VMs&CTs: 156 (+56)

Research work on running HPC in the JINR cloud

- Network bandwith and latency evaluation of various setups in KVM and OpenVZ virtualization technologies
- GPGPU passthrough into KVM VMs and OpenVZ CTs

**Visualization of statistics on resources utilization**

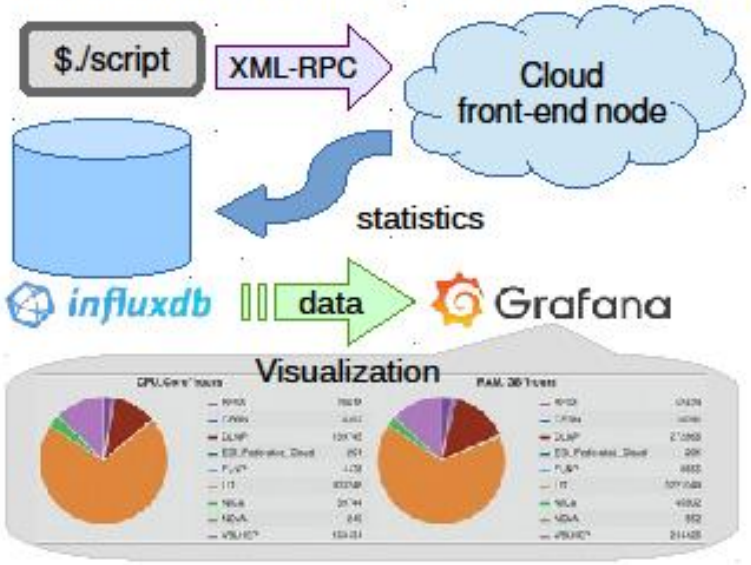


**Increasing number of tasks the JINR cloud is used for**

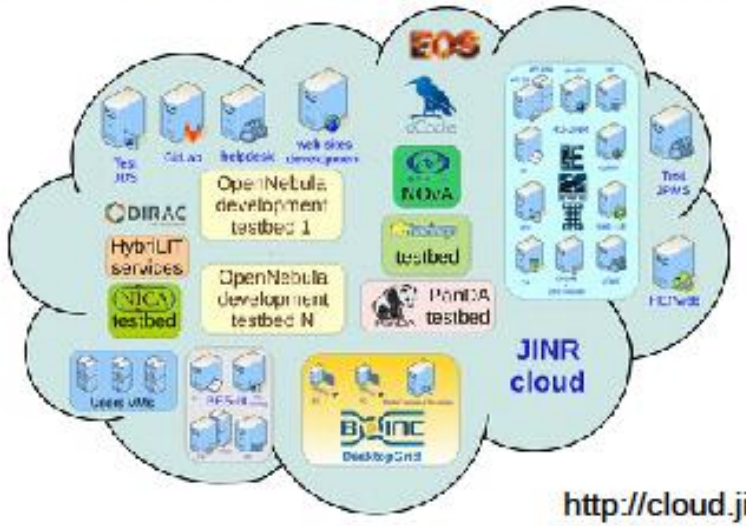


http://cloud.jinr.ru

## HybriLIT components: management, computation, service

Use of virtual machines for hosting managing services. Development of virtual desktops for work with applied software

Computer component has a heterogeneous structure with support for the newest GPU and processors

CERN VM File System is used for management of own software repository

**SLURM**
resource management system suitable for usage on large and small Linux clusters.

**hybrilit.jinr.ru**
Website of heterogeneous cluster HybriLIT.

**Virtual desktops**
Pool of virtual desktops used by users for rich graphical applied software.

**HybriLIT statistics**
service providing payload resource monitoring.

## Cluster infrastructure

**Computation component HybriLIT**

TOTAL RESOURCES
252CPU cores;
77184 CUDA cores;
182 MIC cores;
~2,5 Tb RAM;
~57 Tb HDD.

HARDWARE

SuperBlade Chassis including 10 calculation blades for run user tasks.

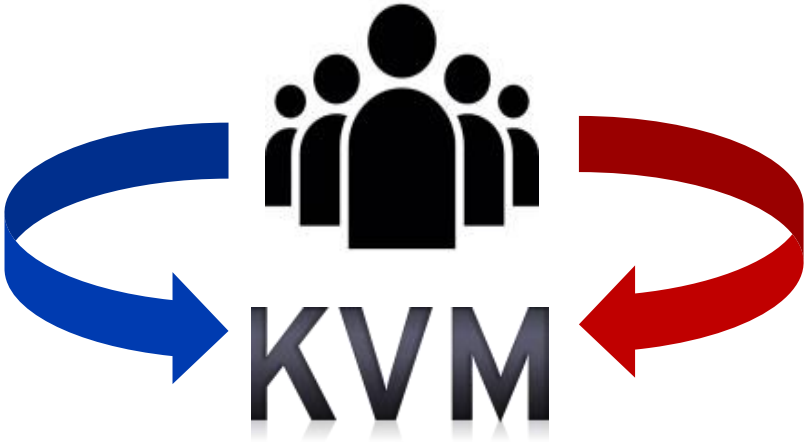


**Virtual Desktops for COMSOL Multiphysics**

48 virtual desktops for users who use COMSOL Multiphysics software and more applied softwar

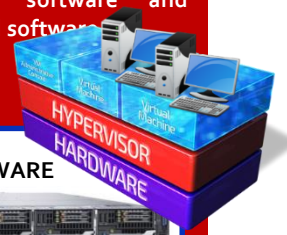


HARDWARE

Based on Dell PowerEdge FC430 including 8 server nodes.

# Simulation of Cloud Computation MPI Applications

A parallel algorithm and corresponding software for parallel computing using MPI technology are developed on the basis of the LIT JINR computer center. To optimize the scheme of parallel computations it is necessary to test the algorithm for various combinations of equipment parameters, number of processors and parallelization levels. Such optimization can be achieved by simulating the MPI computing processes. Results of the MPI computing simulations is presented on the example of calculating long Josephson junctions.

## Simulation Verification

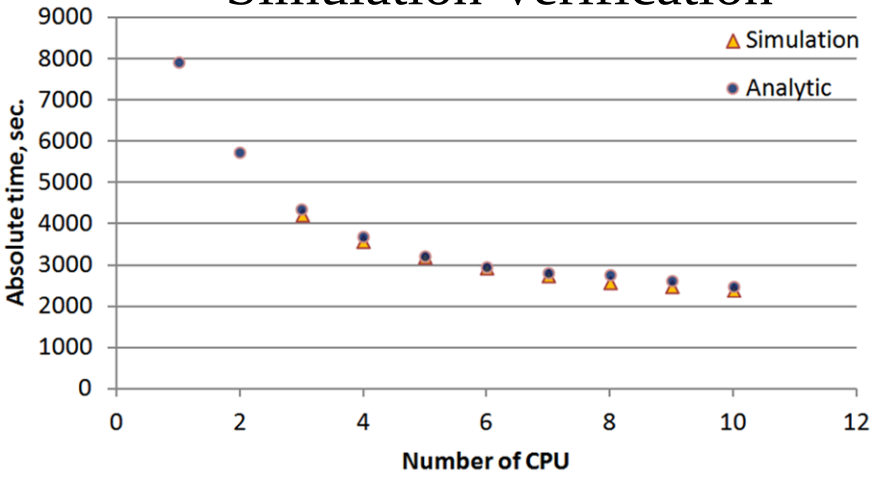


## Simulation Results

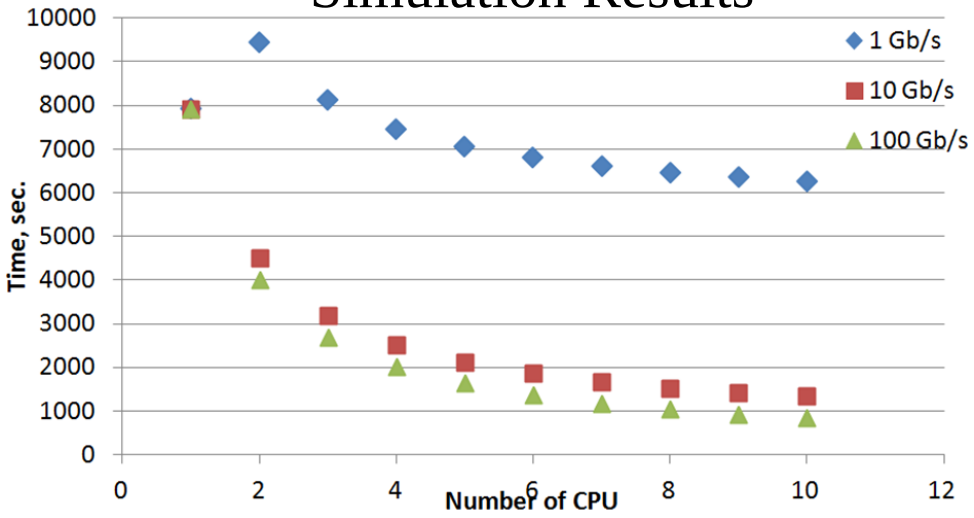


The significant gain in execution time is not observed when the number of processors more than 6. Throughput increasing from 1 Gb/s to 10 Gb/s provides a significant gain in execution time, but its further increase from 10 Gb/s to 100 Gb/s is not useful.

The work was funded by
RFBR project 15–29–01217

G. Ososkov, M. Bashashin, N. Kutovskiy, A. Nechaevskiy, Yu. Shukrinov,
O. Streltsova, D. Podgainy, V. Trofimov, E. Zemlyanaya, M. Zuev, I. Rahmonov

# ASYMMETRIC TRACK-ETCHED SINGLE NANOPORES FOR USE IN THE SENSOR TECHNOLOGY

**K. Olejniczak[1,2], O. L. Orelovitch[1], P. Yu. Apel[1]**

[1]Flerov Laboratory of Nuclear Reactions, Joint Institute for Nuclear Research, Dubna, Russia
[2]Chair of Nuclear and Radiation Chemistry, Nicolaus Copernicus University, Torun, Poland

## INTRODUCTION

Recently, artificial single nanopores have been receiving more and more scientific attention due to their applicability in nanofluidics, sensor technology and information processing. It is known that the ion transport asymmetry is directly related to the geometrical asymmetry of pores. In this work we prepared the single-pore membranes with high ion current rectifiction effect. This property is characteristic of nanopores with a bullet-like-shaped tip. Up to now, the membranes with single bullet-like pore have not been extensively studied. Thus, the aim of this work was to fill this gap by determining the level of uniformity of single asymmetric pores. Such studies are necessary for a better understanding of the electrical behaviour of nanopores and for the development of membrane-based sensors.

## EXPERIMENTAL METHODS

**I. Preparation of single-pore membranes with diode-like properties:**
a) the irradiation of 12 μm polyethylene terephthalate (PET) films with heavy ions (Fig. 1). Two types of film, Hostaphan RN and Hostaphan RNK (biaxially oriented coextruded film), were used in the experiment.
b) physicochemical treatment of irradiated samples to prepare the cylindrical pores with highly-tapered tip:
- the treatment of membranes using UV radiation (24 h on one side of the membrane)
-chemical etching of membranes (conditions: surfactant-doped 5 mol/L NaOH, temperature of 60 °C, time 6 min 30 s).

**II. Current-voltage characteristic of samples in electrolyte solutions**
I-V characteristics of the samples were determined using an electrolytic cell with Ag/AgCl electrodes. Each half-cell was filled with KCl solution. The electric current was measured by stepping the voltage between +1 and -1 V with a PC-controlled Hioki 5322 LCR-meter equipped with a shunt resistor.

**III. The observation of the samples surfaces using Scanning Electron Microscopy (SEM)**

## RESULTS AND DISCUSSION

The shape of the pore channels produced in the ion-irradiated Hostaphan RN is shown in Fig. 2. It is seen that process of track etching in the presence of a surface-active agent allowed to produce asymmetric nanopores with a bullet-shaped mouth. The pore radii on both sides of the membranes were determined from SEM images of the samples with a pore density of $9.7 \times 10^7$ pores/cm$^2$. The average tip and base radii were found equal to 21±1 and 110±4 nm, respectively. The distribution of the tip radii in the investigated membrane is presented in Fig. 3. The nanopores with a tip radius of 17-23 nm predominated.

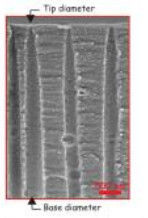


Fig. 2. Cross-section SEM image of Hostaphan RN with pore density of $9.7 \times 10^7$ pores/cm$^2$ etched in surfactant-doped 5 mol/L NaOH.

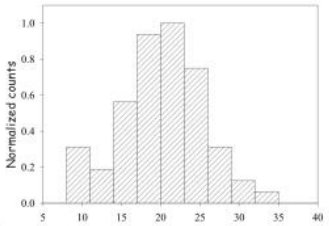


Fig. 3. Tip radius distribution in Hostaphan RN etched in surfactant-doped 5 mol/L NaOH for 6 min 30 s.

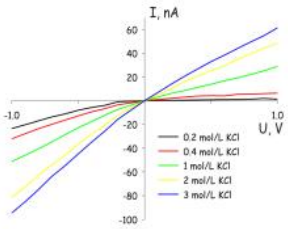


Fig. 4. Current-voltage characteristics of a selected single pore in Hostaphan RN recorded at different KCl concentrations.

The current-voltage responses of a selected single pore in Hostaphan RN recorded for different KCl concentrations are shown in Fig. 4. The biggest ion current rectification effect in all investigated single nanopores was found at electrolyte concentration of 0.2 mol/L. Lower, but still high rectification effect was observed for nanopores filled with the 0.4 mol/L electrolyte solution. In both cases, the shape of the curves was clearly asymmetric showing a diode-like behaviour of negatively charged nanopores.

The uniformity of properties of the single pores in Hostaphan RN and Hostaphan RNK was determined from electro-conductivity data (Table 1). The effective pore radii and rectification ratios of nanopores were measured. Additionally, the reproducibility of these parameters for the same pore was investigated (Table 2).

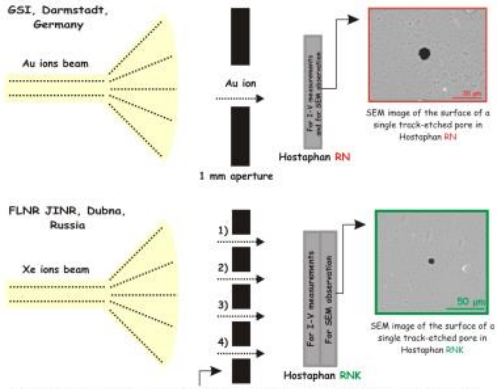


Fig. 1. Preparation of single ion tracks in PET.

Table 1. Rectification ratios I(-|V|)/I(+|V|) at different KCl concentrations and effective pore radii ($a_{eff}$) for single pores in Hostaphan RN and Hostaphan RNK. Five samples of each type of Hostaphan were analyzed. Each of them was measured once.
The effective pore radius is defined as the radius of a cylindrical pore having the same electrical conductance in 1 mol/L KCl at a 0.1V.

| $C_{KCl}$ | Hostaphan RN | | Hostaphan RNK | |
|---|---|---|---|---|
| mol/L | Mean value | Standard deviation | Mean value | Standard deviation |
| 0.2 | 40 | 31 | 15 | 17 |
| 0.4 | 7.4 | 2.5 | 6.4 | 4.8 |
| 1 | 2.1 | 0.6 | 2.0 | 1.1 |
| 2 | 1.9 | 0.2 | 1.4 | 0.1 |
| 3 | 1.7 | 0.2 | 1.4 | 0.4 |
| $a_{eff}$ [nm] | 102 | 7 | 105 | 28 |

Table 2. Rectification ratios I(-|V|)/I(+|V|) at different KCl concentrations and effective pore radii ($a_{eff}$) for the same single pores in Hostaphan RNK. Each sample was measured three times.

| | Hostaphan RNK | | | | | |
|---|---|---|---|---|---|---|
| $C_{KCl}$ | Pore 1 | | | Pore 2 | | |
| mol/L | 1 | 2 | 3 | 1 | 2 | 3 |
| 0.2 | 5.8 | 4.7 | 2.8 | 20 | 40 | 18 |
| 0.4 | 6.8 | 8.1 | 4.6 | 9.7 | 8.7 | 8.9 |
| 1 | 5.4 | 5.2 | 5.9 | 2.5 | 2.6 | 2.7 |
| 2 | 3.2 | 3.2 | 3.4 | 1.3 | 1.3 | 1.3 |
| 3 | 1.8 | 2.0 | 1.9 | 1.2 | 1.2 | 1.9 |
| $a_{eff}$ [nm] | 99 | 103 | 101 | 100 | 120 | 104 |

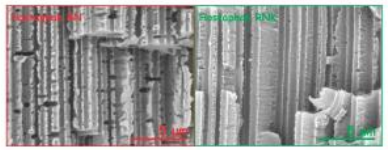


Fig. 5. Difference in morphology of 23 μm thick Hostaphan RN and Hostaphan RNK with pore density of ~ $1 \times 10^7$ pores/cm$^2$. Etching conditions: 2 mol/L NaOH, T = 60 °C, t = 42 min.

As can be seen from Tables 1 and 2, there is a scatter in electrical characteristics from pore to pore and a scatter in electrical characteristics of the same pore from measurements to measurements. For this reason, it is difficult to disentangle geometrical and other, still unknown, factors that cause the non-uniformity of electrical properties of single nanopores. However, the comparison of two types of PET foils seemed to give some hints. We observed a measurable difference between the pores fabricated in Hostaphan RN and Hostaphan RNK. Surprisingly, the pores in the material with smoother pore walls showed a larger scatter in electrical conductance. In the coextruded PET, the filler particles are present only near surfaces while the normal foil (type RN) contains the filler also in the bulk. The filler (presumably silicon dioxide) is an anti-blocking agent added to aid film winding. Apart from the anti-blocking function, the agent particles may influence the crystallization process during the film production. Thus, the morphology of polymer in these two foils – RN and RNK – may significantly differ. This is especially seen after chemical etching which, firstly, reveals alternating crystalline and amorphous domains and, secondly, removes filler particles from the matrix thus creating caverns on the etched surface (Fig. 5). Heterogeneities of this kind result in variations of pore tip size and shape (see histogram in Fig. 3). Moreover, the difference in the degree of surface roughness may cause a difference in effective surface charge density – one of the most important factors affecting the electro-conductive properties of nanopores.

The work was supported by the JINR (grant No. 16-502-03) and the cooperation programme between the Polish scientific institutes with the JINR (No. 04-5-1076-2009/2016). The authors are grateful to the Material Research group (GSI) for providing irradiated samples.

# Studies of Iron and Copper Exposed to Heavy Ion Implantation Using Positron Annihilation Spectroscopy

K. Siemek, P. Horodek, J. Dryzek, A.G. Kobets, V.A. Skuratov, M. K. Eseev, V. I. Hilinov, I. N. Meshkov, O. S. Orlov, A. A. Sidorin

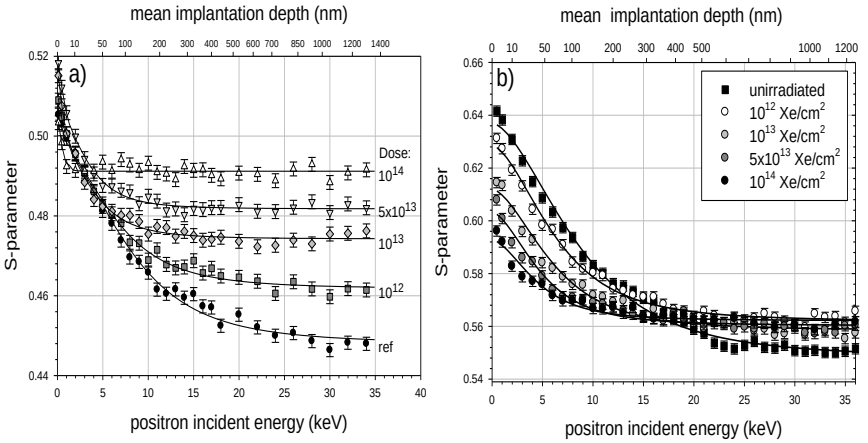


**Fig. 1** The measured annihilation line shape parameter as a function of the positron incident energy for iron a) and copper b) irradiated samples.

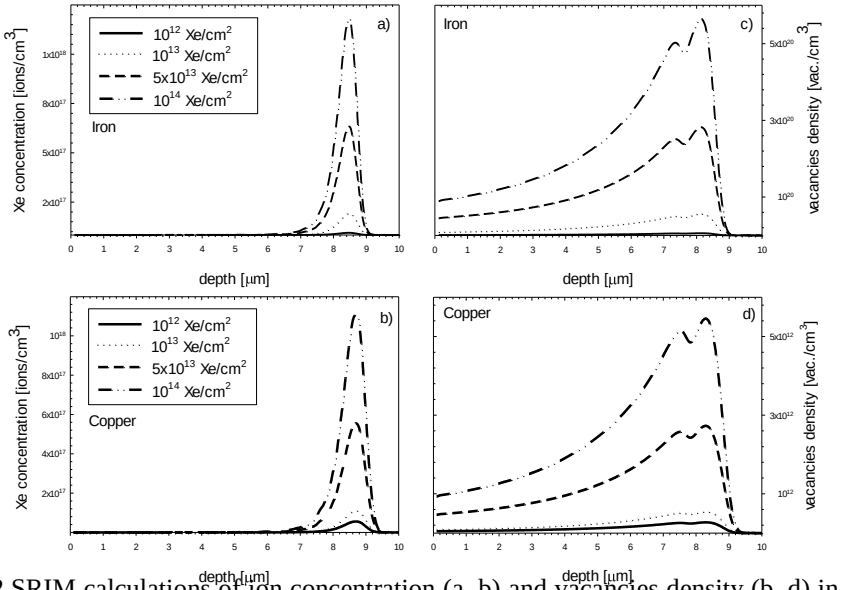


**Fig. 2** SRIM calculations of ion concentration (a, b) and vacancies density (b, d) in dependency on depth after 167 MeV $Xe^{26+}$ implantation with different doses in copper and iron.

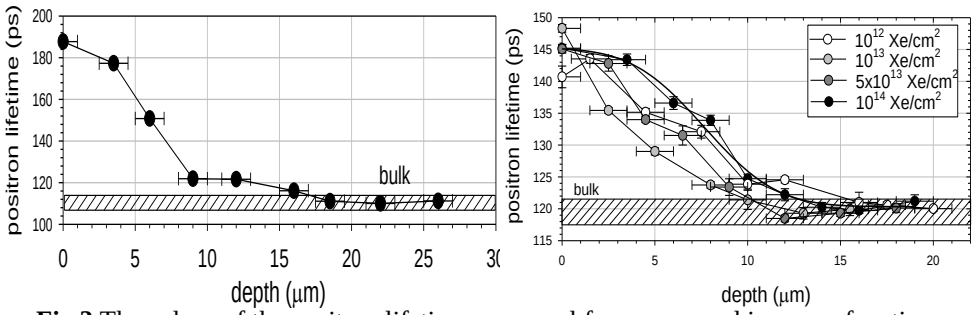


**Fig.3** The values of the positron lifetime measured for copper and iron as a function of the thickness of etched layer from the enter surface.

Irradiation damages were investigated with variable energy positron beam (VEP) and positron lifetime measurements (PALS). The presence of irradiation-induced defects was confirmed in all PAS characteristics. The 167 MeV $Xe^{26+}$ heavy ions with different fluences $10^{12}$, $10^{13}$, $5\times10^{13}$, $10^{14}$ ions/cm$^2$ implanted into samples produce large vacancy clusters and dislocation in the track region. For example in VEP experiments ion implantation caused the shortening of diffusion length. In this way defect concentration depends on the applied dose. For iron samples the depth distribution of the clusters and dislocations is about twice as large as the one predicted by SRIM/TRIM simulations. This can support the long-range effect reported by other authors. However, for copper the measured range of damaged zone was in a good agreement with the one simulated. In this case the "long range effect" observed earlier for copper in other studies was not confirmed.

# Development of Positron Annihilation Spectroscopy at the LEPTA Facility

E. V. Ahmanova, M. K. Eseev, V. I. Hilinov, P. Horodek, A. G. Kobets, I. N. Meshkov, O. S. Orlov, K. Siemek, A. A. Sidorin.

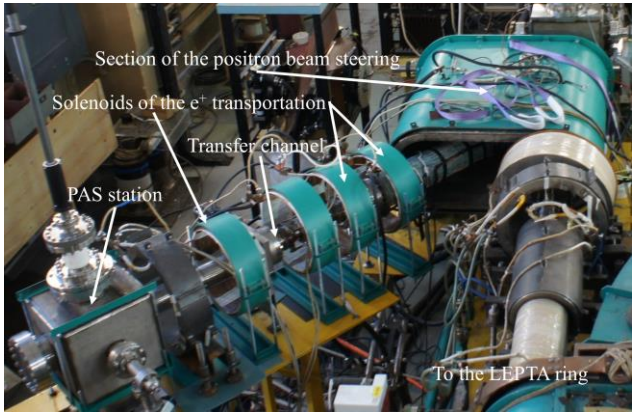


Fig. 1 The positron injector, transfer channel, and PAS station.

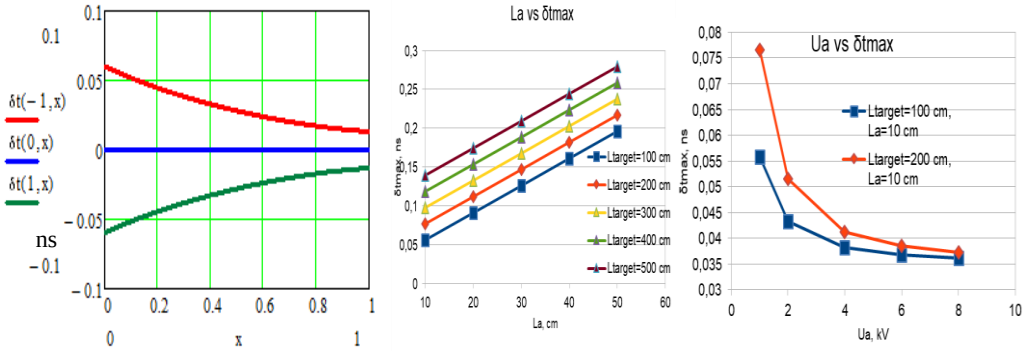


Fig. 3. Simulation of positron dynamic

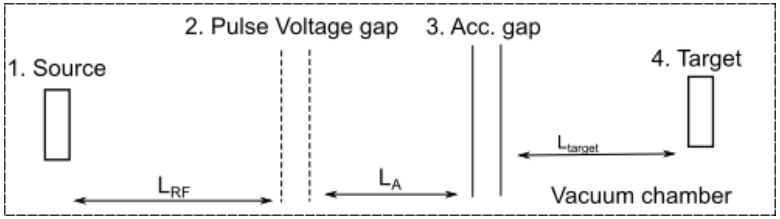


Fig. 2 Scheme of the PALS method, with formation of the ordered positron flux:
1. Cryogenic positron source (Fig. 4); 2. Pulse voltage gap; 3. Acceleration gap (e;ectrostatic field); 4. Target — a sample for PAS studies.

Fig. 4 The autonomus cooling system.

The new positron transfer channel (Fig. 1) was assembled at the LEPTA facility allows us to develop an advanced PAS method — so called «Positron Annihilation Life-time Spectroscopy» (PALS).

Simulation of positron dynamic and selection of optimal parameters for transport channel was done (Fig. 3).

The new monochromatic positron source on the closed loop LHe system is based on $^{22}Na$ isotope tablet of the activity of 30 mCi and cryocooler of the Sumitimo Co. was assembbled and cooled down to 5.3 K. (Fig. 4). Flux of slow monochromatic positrons is achieved of $3.4*10^6$ positrons per second.

# Structural parameters of silver hydrosols: electron microscopy and small angle X-ray scattering

Skoy V.V.[1], Kristavchuk O.V.[1,3], Zabelskii D.V.[2], Lizunov N.E.[3], Trofimov V.V.[3], Soloviov D.V.[2,3], Nechaev A.N.[1,3], Apel P. Yu.[1,3], Kuklin A.I.[2,3]

[1]State University "Dubna", Dubna, Russia
[2]Moscow Institute of Physics and Technology, MIPT, Dolgoprudny, Russia
[3]Joint Institute for Nuclear Research, Dubna, Russia
vskoj@yandex.ru; kuklin@nf.jinr.ru

**Abstract**
In this work we studied the silver hydrosols, i.e. silver water suspensions. The hydrosols samples were investigated on the Rigaku [1] (MIPT, Dolgoprudny, Russia) and BM29 [2] (ESRF, Grenoble, France) instruments by small angle X-ray scattering method. SAXS curves were treated by the Fitter [3] and SasView programs [4]. Images of dried samples of silver hydrosols obtained using a Hitachi SU8020 field emission scanning electron microscope (FESEM) were analyzed. Structural parameters of the suspensions were obtained and polydispersitiy of the silver nanoparticles was estimated using two structural models.

**Introduction**
Silver nanoparticles are widely used in electronic, optical and sensor devices including special substrates for surface-enhanced Raman spectroscopy (SERS). Modification of track-etched membranes with silver nanoparticle is a promising application aimed at fabrication of flow-throw SERS substrates with high sensitivity to different analytes including biologically important molecules. Reproducible fabrication of SERS substrates requires detailed knowledge of nanoparticles' properties such as size distribution, surface charge, content of agglomerates, and others.

**Experimental results**
Here we show the results of studies on silver hydrosols samples by methods of small angle X-ray scattering (Fig. 1) and the results of studies on dried samples by methods of electron microscopy. The silver hydrosols were prepared using electric discharge technology [5]. The silver particles are formed due to the dispersion of the electrode metal in a high-current discharge between closely spaced silver electrodes and further transfer of dispersed silver particles in water. The dried samples of silver particles for electron microscopy investigations were obtained by precipitation of silver hydrosols on membranes. Polyethylene terephthalate track-etched membranes were modified with polyethyleneimine and then coated with Ag nanoparticles. An FESEM image of membrane surface covered with silver particles is presented in Fig. 2 and a relevant histogram is shown in Fig. 3.

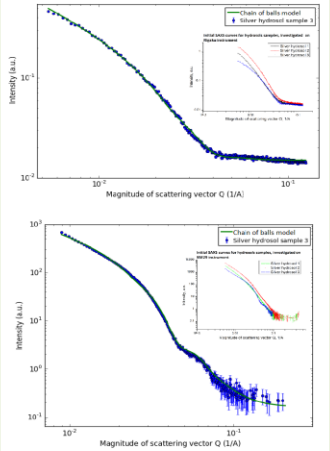


Fig. 1 Fitting of SAXS curves for silver hydrosol samples using the chain of balls model.

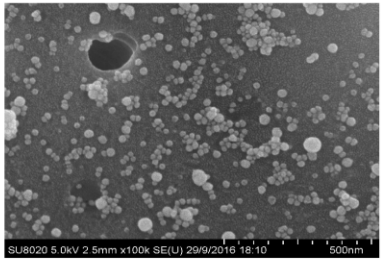


Fig. 2 FESEM image of silver nanoparticles on track-etched membrane.

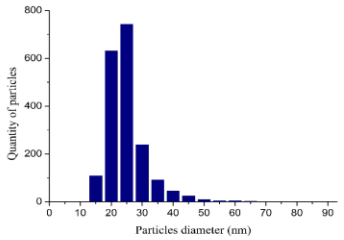


Fig. 3 Histogram of silver particles diameters distribution.

**Modeling and conclusion**
Triaxial ellipsoids and chain of balls models were shown to be the best fits for the shown above SAXS curves for silver hydrosols samples. For the chain of balls model fit parameters of 5.0, 7.1 and 8.6 nm as radii, with 50%, 30% and 20% polydispersity, respectively, for three different samples of suspension were obtained. The applicability of this model probably shows that significant portion of silver nanoparticles aggregate in the solution (and not only on surface of the substrate used for FESEM examination). It was found that the fitting parameters were slightly different for the SAXS curves obtained on the two different instruments (Rigaku and BM29). Possible reasons for the difference are heterogeneity of the studied hydrosols and their degradation.

**References**
[1] T. N. Murugova, A. V. Vlasov, O. I. Ivankov, et al. J. Optoelectron. Adv. Mater. 17 (2015) 1397–1402.
[2] A. Round, E. Brown, R. Marcellin, et al. Acta Crystallogr. Sect. D Biol. Crystallogr. 69 (2013) 2072–2080. doi:10.1107/S0907444913019276.
[3] http://yumo.jinr.ru/software/fitter
[4] http://www.sasview.org/index.html
[5] N. N. Ostroukhov, A. Yu. Tyanginskii, V. V. Sleptsov, and M. V. Tserulev. Inorganic Materials: Applied Research, 2014, Vol. 5, No. 3, pp. 284–288.

# "Structure and formation threshold of latent tracks in $Al_2O_3$ irradiated with swift heavy ions"

R. A. Rymzhanov, N.A. Medvedev, A.E. Volkov, V.A. Skuratov

A combined theoretical and experimental investigation of latent tracks in $Al_2O_3$ crystals was performed.

MD simulation

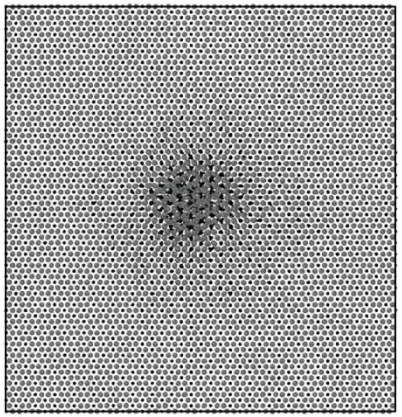

TEM image

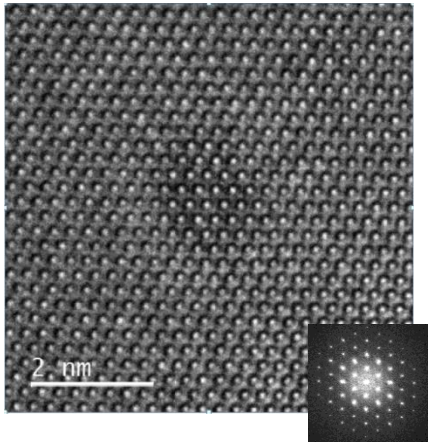


Calculated track formation threshold

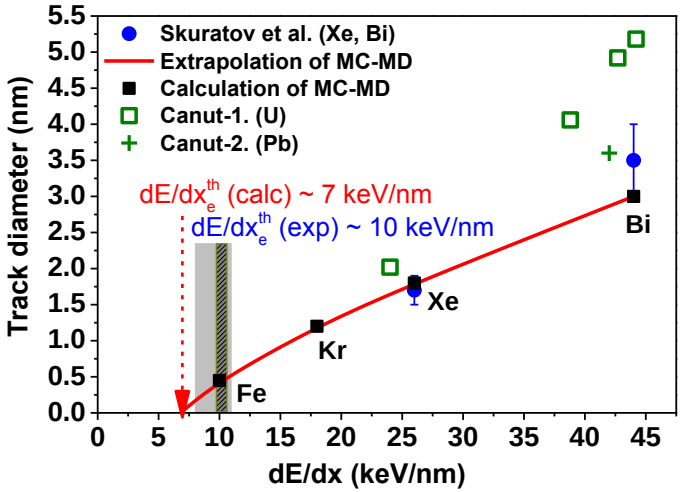


- TEM and MD agree on track size & structure
- The energy loss threshold of track formation in $Al_2O_3$ is ~ 7 keV/nm)
- Al sublattice in SHI track is damaged stronger than O sublattice
- The saturation can be can explained by partial annealing of ion tracks during their interference

Simulation of X-ray diffraction patterns

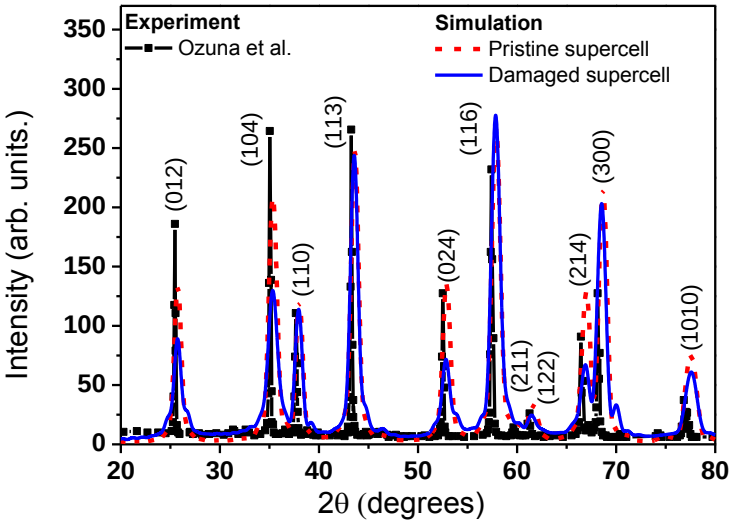

# Heterogeneous cluster HybriLIT: IT-ecosystem

Matveev M., Belyakov D., Podgainy D., Torosyan Sh., Vala M., Valova L., Zaikina T.

***In order to increase the efficiency of work on the heterogeneous cluster HybriLIT, there appears a need to develop and support an information-computing environment for work with parallel programming technologies used in the process of developing high performance applications and carrying out computations by means of resources of the heterogeneous cluster.***

Software and information environment to provide users with possibility to use the resources of the cluster

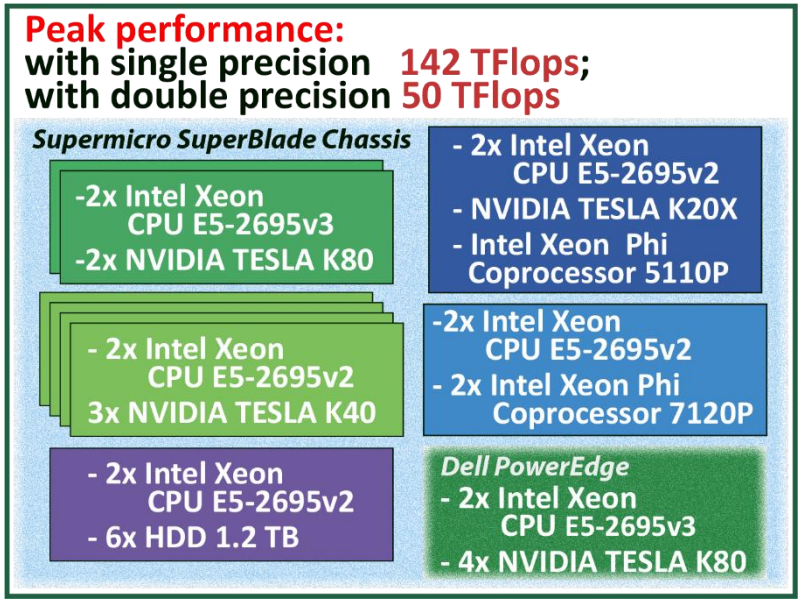


Regular tutorials on parallel programming technologies held by the HybriLIT team

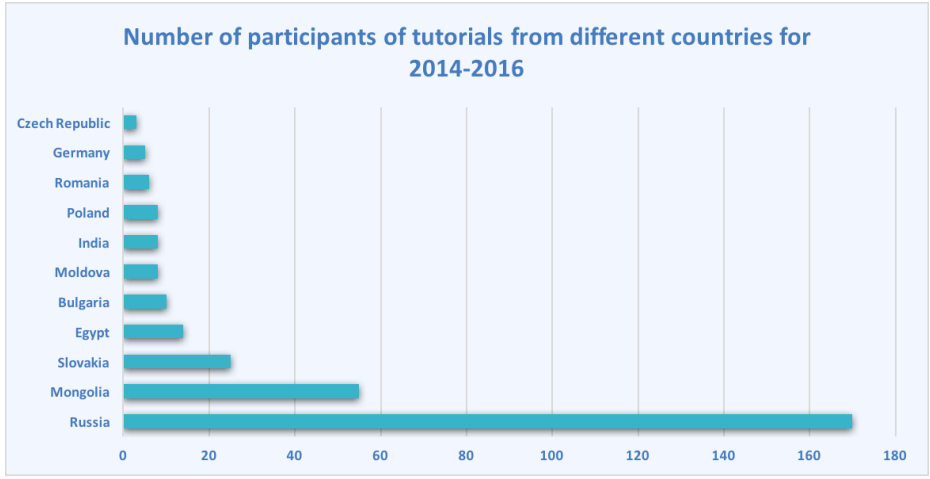


During 2014-2016, there were held 53 tutorials and lectures in which more than 350 scientists, specialists and students from JINR, other Russian scientific centers and JINR Member States participated

# Data Management of the Environmental Monitoring Network: UNECE ICP Vegetation Case

Authors: Gennady Ososkov, Marina Frontasyeva, Alexander Uzhinskiy, Nikolay Kutovskiy, Boris Rumyantsev, Andrey Nechaevsky, Sergey Mitsyn, K. Vergel

UNECE ICP Vegetation programme is realized in 36 countries of Europe and Asia. Mosses are collected at thousands of sites across Europe and Asia. The goal of this programme is to identify the main polluted areas, produce regional maps and further develop the understanding of long-range transboundary pollution.

Since 2014 FLNP (Frank Laboratory of Neutron Physics) at the Joint Institute for Nuclear Research has been in charge of that part of the project which is related to the moss biomonitoring

The ICP Vegetation programme is very important project, but it has a serious weakness related to its weak adoption of modern informational technologies.

Right now information on collecting and processing of samples is carried out manually or with minimum automation. There is no common standards in data transfer, storing and processing software. The situation affects quality, effectiveness and speed of research.

The aim of the project is to create cloud platform using modern analytical, statistical, programmatic and organizational methods to provide the scientific community with unified system of collecting, analyzing and processing of biological monitoring data.

Parts of the project have already been implemented. Public and private part of the portal is available at moss.jinr.ru Fully functional platform is going to be implemented in the next two years

# Analysis of the new possibilities of using Intel Xeon Phi processors for solving application programs

Adam Gh., Alexandrov E., Bashashin M., Matveev M., Podgainy D., Streltsova O., Zemlyanaya E., Zuev M.

## Test on the basis of GIMM_FPEIVE package

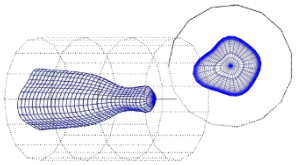

The complex GIMM_FPEIVE is intended for modeling thermo-physical processes under irradiation of materials with ion beams.

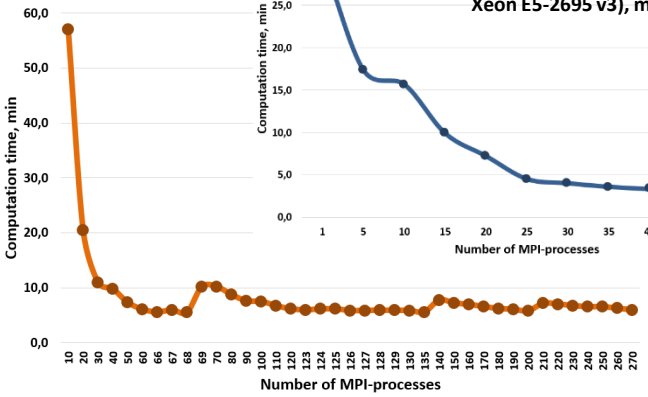


## Test on numerical solving the system of polaron equations

Solvated (hydrated) electron states are of the utmost interest to modern science due to their special physical and chemical properties. The software implementation is based on the MPI technology

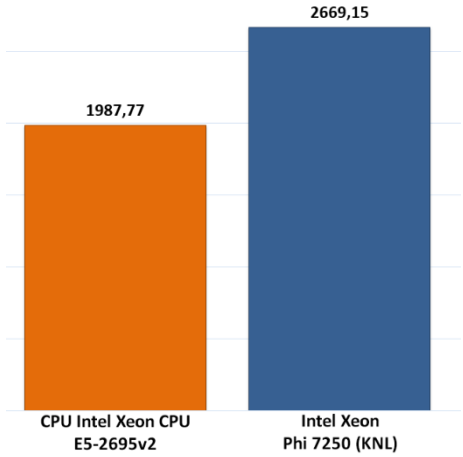


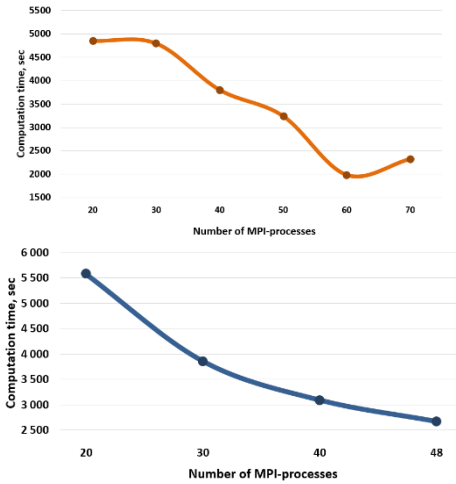


## Results of Linpack benchmark

Linpack benchmark test detects the performance of the whole computational system as well as of the parts of its components. However, its main target to assess performance based on the solution of the SLAE, $Ax=f$, by means of LU-factorization with partial pivoting has remained. Nowadays, this test is used for the performance evaluation of the supercomputers included in TOP500. The efficiency is defined as the ratio of the obtained result of the test to the theoretical value given by the manufacturer.